A Numerical Study of Flow Circulations in the Central Valley of California and Formation Mechanisms of the Fresno Eddy

YUH-LANG LIN AND I-CHUN JAO*

Department of Marine, Earth and Atmospheric Sciences, North Carolina State University, Raleigh, North Carolina

(Manuscript received 27 February 1995, in final form 30 May 1995)

ABSTRACT

In this study, the authors have conducted a series of numerical experiments to investigate the flow circulations in the Central Valley of California and the formation mechanisms of the Fresno eddy. The authors have found the following:

• Under an adiabatic northwesterly, low–Froude number flow over the Central Valley, two cyclonic vortices form in the basin. One is located on the lee slope of the northern Coastal Range, while the other is located to the south of the San Joaquin Valley. The first may be identified as the Sacramento eddy, while the second may be identified as the Fresno eddy, although the Fresno eddy is located slightly farther to the south. The formation of the Sacramento eddy may be explained by either the generation of potential vorticity (Smith) or the generation of vorticity due to baroclinicity (Smolarkiewicz and Rotunno) on the lee slope in a low–Froude number flow. The Sacramento eddy may also be classified as a lee mesocylone since it is collocated with a lee mesolow (Lin et al.). In addition, a northwesterly jet forms at the gap of the Coastal Range due to the channeling effect.

• The Fresno eddy forms when the low–Froude number northwesterly flow meets the return flow from the Tehachapi Mountains in a rotating fluid system and is strengthened and expands farther to the north due to the effects of nocturnal radiative cooling. The northwesterly jet in the Central Valley, the southeasterly wind from the foothills of the Sierra Nevada, and the blocking effect due to the Tehachapi Mountains all play important roles in the formation of the Fresno eddy. The Sacramento eddy moves eastward to the foothills of the Sierra Nevada, while the jet at the gap of the Coastal Range is suppressed when nocturnal radiative cooling is present.

• The nocturnal drainage flow over the western slope of the Sierra Nevada is weakened by the southerly return flow from the Tehachapi Mountains. The simulations indicate that in the absence of nocturnal radiative cooling the Fresno eddy still forms but is weaker and is located near the southern end of the San Joaquin Valley.

• The Fresno eddy will form in an environment characterized by low–Froude number northwesterly wind. Suitable incoming flow speed and direction are among the major factors in determining the formation and strength of the Fresno eddy.

• The return flow from the southern boundary of the San Joaquin Valley plays an important role in the formation of the Fresno eddy.

• The Fresno eddy does not form in the absence of planetary rotation.

• The β effect plays a negligible role in the formation of the Fresno eddy.

1. Introduction

Understanding the dynamics of the flow circulation in the Central Valley of California is important since the circulation controls the distribution of air pollutants in this region. During the summers of 1990 and 1991, the San Joaquin Valley Air Quality Study (SJVAQS) and the Northern California Transport Experiments were conducted to study the wind patterns thought to play major roles in the air quality of the Central Valley. The Fresno eddy, which develops in the San Joaquin Valley, is a combination of the southeasterly wind along the foothills of the Sierra Nevada and the northwesterly jet in the central part of the basin (e.g., Blumenthal et al. 1985). The mesoscale wind pattern associated with the Fresno eddy is considered to play an important role in influencing the air quality in the San Joaquin Valley.

Figure 1a shows the topographic features of the Central Valley. The San Joaquin and Sacramento Valleys are surrounded by the Coastal Range to the west and the Sierra Nevada to the east. The whole basin area is approximately 600 km long and 100 km wide, while the San Joaquin Valley in the southern end of the basin is approximately 400 km long. The Coastal Ranges are about 0.6–1.0 km high, while the southern (northern) Sierra Nevada are about 3.0–4.0 (1.5–2.5) km high. The major break in the Coastal Range is located in the

* Current affiliation: Department of Atmospheric Science, National Central University, Chung-Li, Taiwan.

Corresponding author address: Prof. Yuh-Lang Lin, Department of Marine, Earth and Atmospheric Sciences, North Carolina State University, Raleigh, NC 27695-8208.

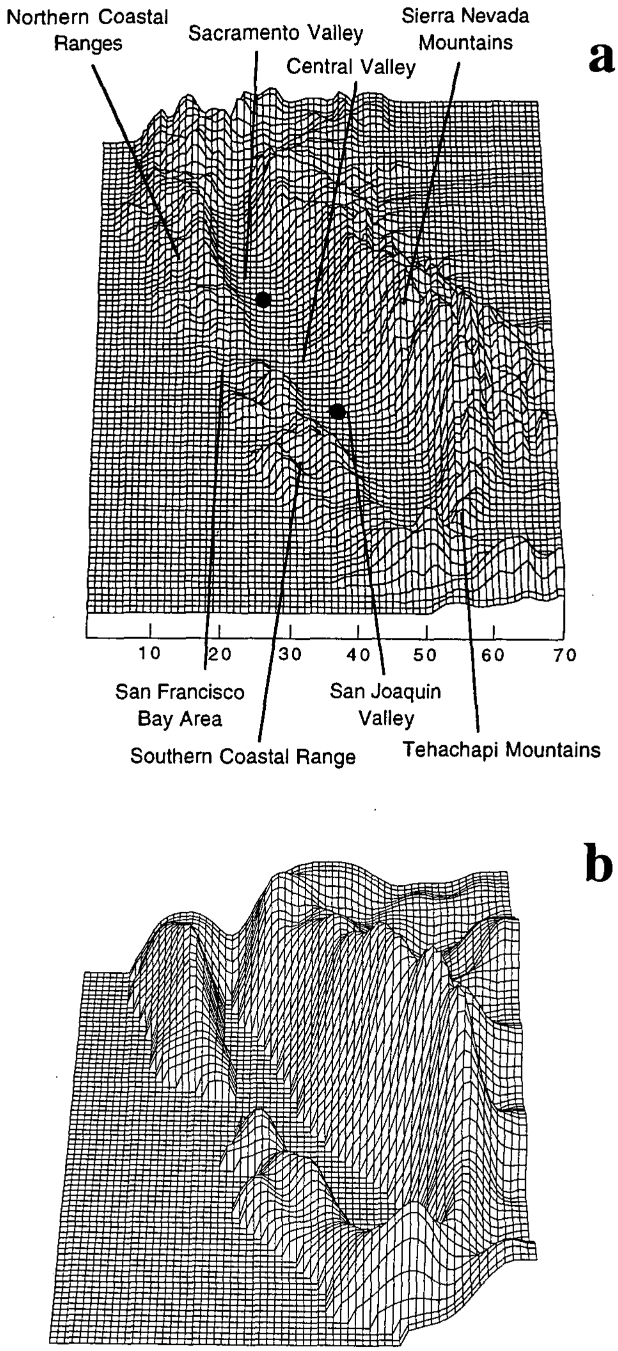

FIG. 1. (a) The topographic features of the Central Valley. The scale at the bottom of the figure is normalized by 10 km. The dot in the Sacramento Valley denotes Sacramento, while the one in the San Joaquin Valley denotes Fresno. (b) The smoothed topography used for all experiments in this study. Notice that we have used a different vertical scale in plotting (b).

San Francisco Bay area. The break provides a channel for air to flow from the Pacific Ocean into the San Joaquin Valley. The Tehachapi Mountains tend to block the flow in the southern end of the San Joaquin Valley, although part of the air tends to flow out of the valley at the Tehachapi Pass.

During the summer months, the North Pacific high pressure system produces a predominantly northwesterly flow with an approximate near-surface wind speed of 7 m s^{-1} upstream of the Coastal Range. Over land, the airflow is strongly influenced by the complex topography and the diurnal cycle of solar heating and cooling. The climate in the basin during the summer is characterized by warm, dry days and relatively cool nights, with clear skies and decreased rainfall (Ruffner and Bair 1985). Strong nocturnal radiative cooling occurs over these mountains. The Coastal Range blocks the large-scale flow, limiting the entrance of maritime air into the basin. Strong channeling of maritime air occurs near the San Francisco Bay area, and the flow partly penetrates southward (northward) into the San Joaquin (Sacramento) Valley. Four major mesoscale flow features are observed in the San Joaquin Valley. 1) A northwesterly low-level jet (LLJ) is observed in the Central Valley during the night. The LLJ reaches its maximum wind speed in the late evening and dissipates during the morning hours. 2) The Fresno eddy is located in the San Joaquin Valley. Observations indicate that this mesoscale eddy develops during the morning hours when there exists a strong low-level wind from the southeast. The depth of the eddy circulation may reach a height of 1 km. It dissipates during the early afternoon. 3) Downslope winds are evident over a shallow layer in the southern end of the valley. 4) A sea-breeze circulation penetrates into the valley during the evening hours, while a land breeze occurs at night. Tanrikulu and McNider (1992) observed the penetration of the sea breeze into the Central Valley on 3–4 August, 1990 during SJVAQS. The prevailing synoptic conditions and the above mesoscale wind patterns are described in detail in other studies (e.g., Tanrikulu and McNider 1992; Neff et al. 1992; Wilczak et al. 1992).

As mentioned earlier, since the Fresno eddy is considered to play an important role in influencing the distribution of air pollutants in the Central Valley, it is essential to understand its formation mechanisms. Previous studies have raised questions concerning the physical mechanisms responsible for the formation of the Fresno eddy. Four mechanisms have been suggested (summarized in Neff et al. 1992). 1) The southeasterly flow, which develops between midnight and early morning, reflects a topographic deflection of the Central Valley jet as it reaches the southern end of the San Joaquin Valley. 2) Nocturnal drainage flow generated on the slopes of the Sierra Nevada. 3) Kelvin waves propagating along the Sierra Nevada. The distance the southeasterly wind flows and the wind speed within the side canyons is sufficient for the Coriolis force to deflect drainage winds from the Sierra Nevada toward the northwest. 4) The Fresno eddy owes its existence to the variation of the Coriolis force with latitude (β effect). Mesoscale wind patterns in the San Joaquin Valley have been analyzed by Neff et al. (1992) and Wilczak et al. (1992), among others. They showed that when an LLJ is present in a southeasterly surface flow, the Fresno eddy is observed to develop, but when the surface flow is northwesterly, the Fresno eddy is weak or nonexistent. Seaman and Stauffer (1994) used the The Pennsylvania State University–National Center for Atmospheric Research MM5 model to simulate mesoscale flow circulations in the San Joaquin Valley. They found that the Fresno eddy forms in the San Joaquin Valley during the night primarily due to the combination of blocking effects associated with the terrain and stable marine air that is advected inland. However, a systematic sensitivity test of the flow response to influential factors, such as basic flow speed and direction, diabatic forcing associated with radiative cooling, the effects of the southern boundary, and planetary rotation, etc., is still needed. In this study, we simulate and discuss the flow circulation in the entire Central Valley, instead of just a portion of the basin as simulated by other researchers in earlier studies.

Similar phenomena have also been found in southern California, such as the midchannel eddy over the Santa Barbara channel (e.g., Kessler and Douglas 1991). During the night, strong radiative cooling occurs over the eastern part of the terrain along the coastline and induces a significant easterly downslope flow that appears to be associated with the onset of the midchannel eddy. Although the scale of the midchannel eddy is larger than the scale of the Fresno eddy, one may postulate that the sequences of formation events are similar. A number of studies have been conducted on valley drainage winds. It has been proposed that the driving force for drainage (downslope) flow is the buoyancy force generated by nocturnal radiative cooling of the layer adjacent to the slope. The impact of drainage winds has been found in various places, such as Grand Mesa, Colorado (King et al. 1990; Whiteman 1990); Rattlesnake Mountain, Washington (Horst and Doran 1986, 1988); and Brush Creek Valley, Colorado (Barr and Orgill 1989; Doran 1990; Orgill et al. 1990). Since the drainage flow has been hypothesized to be an important factor in the formation of the Fresno eddy, the effect of nocturnal radiative cooling will be investigated in this study. In addition, the dependence of drainage flow and its relation to the formation of the Fresno eddy will also be examined by varying the characteristics of the ambient environment, such as basic wind speed and direction.

The objectives of this paper are to study the mesoscale circulations in the Central Valley and the formation mechanisms of the Fresno eddy. Since the combined orographic and thermal forcing are extremely complicated in the San Joaquin Valley, we will take a systematic approach that allows us to isolate and thoroughly study individual physical processes. Due to the highly nonlinear characteristics of the flow in the valley, the corresponding mathematical problem becomes complicated and is analytically intractable. Therefore, we use a simple, theoretically oriented nonlinear numerical model to study the flow dynamics. This type of idealized model provides a great deal of flexibility in varying different dominant flow parameters, such as the Froude number, height of the Tehachapi Mountains, ambient wind speed and direction, and strength and duration of the diurnal thermal forcing.

The major features of the numerical model used in this study will be briefly described in section 2. In section 3, the flow circulation in the Central Valley and the formation of the Fresno eddy will be discussed. On the basis of the results presented in section 3, certain sensitivity tests will be made in section 4 to examine individual physical processes. Conclusions are given in the last section.

2. The numerical model

The model used in this study is based on a three-dimensional, hydrostatic, Boussinesq fluid system. The momentum, thermodynamic energy, incompressible continuity, and hydrostatic equations in terrain-following coordinates are given by

$$\frac{\partial u}{\partial t} + (U+u)\frac{\partial u}{\partial x} + (V+v)\frac{\partial u}{\partial y} + \dot{\sigma}\left(\frac{\partial U}{\partial \sigma} + \frac{\partial u}{\partial \sigma}\right) - (f_0 + \beta y)v + \left[\frac{\partial \phi}{\partial x} + \left(\frac{\sigma - z_T}{z_T - z_s}\right)\frac{\partial z_s}{\partial x}\frac{\partial \phi}{\partial \sigma}\right] = -\nu u \quad (1)$$

$$\frac{\partial v}{\partial t} + (U+u)\frac{\partial v}{\partial x} + (V+v)\frac{\partial v}{\partial y} + \dot{\sigma}\left(\frac{\partial V}{\partial \sigma} + \frac{\partial v}{\partial \sigma}\right) + (f_0 + \beta y)u + \left[\frac{\partial \phi}{\partial y} + \left(\frac{\sigma - z_T}{z_T - z_s}\right)\frac{\partial z_s}{\partial y}\frac{\partial \phi}{\partial \sigma}\right] = -\nu v \quad (2)$$

$$\frac{\partial \theta}{\partial t} + (U+u)\frac{\partial \theta}{\partial x} + (V+v)\frac{\partial \theta}{\partial y} + u\frac{\partial \Theta}{\partial x} + v\frac{\partial \Theta}{\partial y} + \dot{\sigma}\frac{\partial(\Theta + \theta)}{\partial z} = \frac{\theta_0}{c_p T_0}Q - \nu\theta \quad (3)$$

$$\frac{\partial}{\partial x}[(z_T - z_s)u] + \frac{\partial}{\partial y}[(z_T - z_s)v] + \frac{\partial}{\partial \sigma}[(z_T - z_s)\dot{\sigma}] = 0 \quad (4)$$

$$\frac{\partial \phi}{\partial z} = g\frac{\theta}{\theta_0}\left(\frac{z_T - z_s}{z_T}\right), \quad (5)$$

where the variables are defined as

t time
x horizontal coordinate in east–west direction
y horizontal coordinate in north–south direction
σ vertical coordinate
U horizontal basic wind velocity in x direction
V horizontal basic wind velocity in y direction
u horizontal perturbation wind velocity in x direction
v horizontal perturbation wind velocity in y direction
$\dot{\sigma}$ perturbation vertical wind velocity in σ coordinate
ϕ kinematic pressure (p/ρ_0)
Θ basic potential temperature
θ perturbation potential temperature
T_0 constant reference temperature
θ_0 constant reference potential temperature
g gravitational acceleration
ν coefficients of Rayleigh friction and Newtonian cooling
f_0 Coriolis parameter (constant)
β $=df/dy$; meridional gradient of the Coriolis parameter (constant)
z_T top of the computational domain
z_s terrain height
c_p specific heat capacity of dry air at constant pressure
Q diabatic heating rate per unit mass (J kg^{-1} s^{-1}).

The model has the following characteristics:

- The leapfrog scheme is used for time marching.
- A fourth-order centered-difference scheme is used for horizontal space derivatives.
- A second-order centered difference is used for vertical space derivatives.
- The lower boundary condition is $\dot{\sigma} = 0$.
- The upper radiation boundary condition is approximated by a sponge layer (Klemp and Lilly 1978).
- A zero-gradient lateral boundary condition is applied, which allows gravity waves generated in the computational domain to propagate out of the lateral boundaries.
- A five-point numerical smoother (Shapiro 1970) is applied at every time step in both the horizontal and vertical directions, while a three-point smoother (Asselin 1972) is applied in time.

The details of the numerical model can be found in Weglarz (1994). The basic wind (U, V) is assumed to be independent of x, y, and σ in this study. The real topography, which cuts through the atmosphere without modifying the initial fields, is then introduced. Since the atmosphere is rather stable in the basin at night during summer, we assume a stable stratification characterized by a constant Brunt–Väisälä frequency of 0.01 s^{-1} for all experiments discussed here. The Coriolis effects are included in the model by making either the f- or β-plane approximations, depending upon the particular case being simulated. The reference Coriolis parameter f_0 is set to 8.8×10^{-5} s^{-1}, since the center of the basin is located roughly at 37°N. The flow is assumed to be inviscid in the physical domain (i.e., $\nu = 0$ for $z \leq 10$ km). The upper third ($10 < z \leq 15$ km) of the computational domain is the sponge layer. The horizontal grid interval in both x and y directions is 10 km, while the vertical grid interval is 500 m. The total number of model grid points in the x, y, and z directions are $65 \times 75 \times 31$, respectively. The time interval is 20 s. Figure 1b shows the smoothed topography used in this study. The primary mountain peak located in the southern Sierra Nevada is approximately 3173 m in elevation.

A number of simulations have been conducted in this study. All experiments are performed for 22 h. During the first 10 h, the flow is adiabatic ($Q = 0$), and geostrophic adjustment processes have yielded a quasi-steady state by the end of this time period. For times greater than this, and only for those experiments with diabatic forcing, prescribed cooling (which is taken to physically represent the effects of nocturnal radiative cooling) is added for the last 12 h over the mountains. The cooling rate is a linear function of local elevation and decays exponentially above the ground with an e-folding value of 1 km. The maximum cooling rate is -0.2 J kg^{-1} s^{-1}. This is equivalent to -1.0°C h^{-1}, which is estimated roughly from the data collected in the SJVAQS/AUSPEX field experiments (S. Tanrikulu 1993, personal communication). These experiments are summarized in Table 1.

3. Flow circulations in the Central Valley and formation mechanisms of the Fresno eddy

A control experiment (case 1) characterized by a basic wind $(U, V) = (5, -5$ m s$^{-1})$ from the northwest is performed for 22 h. The low-level diabatic cooling is incorporated into the model during the last 12 h by the prescribed thermal forcing term, so that the relationship between the nocturnal drainage flow and the formation of the Fresno eddy can be explored. This allows us to investigate the general flow circulation in the Central Valley and the development of the Fresno eddy. The Froude number is about 0.7 when the upstream basic wind impinges on the Coastal Range but decreases to 0.2 by the time the flow impinges on the Sierra Nevada. The Froude number is defined as $\mathrm{Fr} = U/Nh$, where N and h are the Brunt–Väisälä frequency of the basic flow and the mountain height, respectively. In the above estimate of Fr, we have used $U = 7$ m s^{-1}, $N = 0.01$ s^{-1}, and $h = 1$ km for the Coastal Range, and $h = 3.5$ km for the Sierra Nevada. Generally speaking, it can be considered as a low-Froude number flow in which the effects of nonlinearity are very strong. Notice that the strength of the nonlinearity is controlled by the reciprocal of Fr (e.g.,

TABLE 1. Summary of numerical experiments.

Case	Factors considered	U, V (m s^{-1})	f (s^{-1})	β (m^{-1} s^{-1})	Figures
1	Control case	(5, −5)	8.8×10^{-5}	0	2–4
2	No cooling	(5, −5)	8.8×10^{-5}	0	5
3	Lower southern boundary	(5, −5)	8.8×10^{-5}	0	6
4	Weak wind	(1, −1)	8.8×10^{-5}	0	7
5	Westerly wind	(7, 0)	8.8×10^{-5}	0	8
6	No rotation	(5, −5)	0	0	9
7	With β effect	(5, −5)	8.8×10^{-5}	1.8×10^{-11}	10

Smith 1979). In this control experiment, we assume that the flow is on an f plane.

Figure 2 shows the flow fields after the first 10 h of simulation. The incoming wind is significantly blocked and deflected by the Coastal Range, and a weak reversed flow forms near the surface on the upslope side of the northern Coastal Range (Fig. 2a). Flow splitting is evident upstream of the five peaks of the Coastal Range. Air parcels decelerate over the western slopes of the Sierra Nevada, while they accelerate over eastern and northern slopes, as well as over the Tehachapi Mountains. As can be seen, a region of high winds, which also represents a strong confluence zone, appears to the north. A northwesterly jet occurs at the break of the Coastal Range due mainly to the channeling effect. This jet enters the basin and then splits into two branches: one branch turns northward and forms a well-organized cyclonic vortex in the Sacramento Valley, while the other branch penetrates farther southward down into the San Joaquin Valley and then recirculates since it is blocked by the Tehachapi Mountains at the southern end of the San Joaquin Valley. The vortex in the Sacramento Valley may be called the Sacramento eddy, which appears to be formed by either the generation of potential vorticity (Smith 1989) or by the baroclinically generated vorticity on the lee slope under a low–Froude number flow (Smolarkiewicz and Rotunno 1989). According to Smolarkiewicz and Rotunno (1989), when the Froude number is less than 0.5, a zone of flow reversal on the windward side and a pair of lee vortices with a warm core on the downwind side will appear simultaneously. Higher–Froude number flows have also been found to be able to produce lee vortices (Lin et al. 1992). These types of mesoscale lee vortices have also been simulated in numerical simulations of inviscid, low–Froude number barotropic flow past Hawaii (Smolarkiewicz et al. 1988), the Colorado Rockies near Denver (Crook et al. 1990), and Taiwan (Sun et al. 1991; Lin et al. 1992). In the Taiwan case, Lin et al. (1992) also found that the cyclonic vortex is collocated with the mesolow and may therefore be classified as a mesocyclone. For the present case, the vortex center is also collocated with the mesolow (Fig. 2d). *Thus, the Sacramento eddy may also be classified as a mesocyclone.*

Another cyclonic vortex forms near the southern portion of the San Joaquin Valley and may be identified as the Fresno eddy, even though it is located south of Fresno. Unlike the Sacramento eddy, the Fresno eddy may not be viewed as a mesocyclone since the mesovortex is not collocated with any mesolow (Fig. 2d). This vortex appears to be formed by the flow passing through the gap in the Coastal Range and impinging on the return flow from the Tehachapi Mountains in the lower San Joaquin Valley. It appears that the flow decelerates significantly as it impinges on the western slopes of the Sierra Nevada since the Froude number becomes smaller. There exist three regions of large positive relative vorticity (regions shaded): one in the northern Sacramento Valley, one associated with the Sacramento eddy, and one associated with the Fresno eddy (Fig. 2a). Figure 2b shows the vertical cross section of vector wind and isentropes at $y = -100$ km. A stagnation point and reversed flow exist near the surface over the western slope of the Sierra Nevada at this time. Tanrikulu and Soong (1990) also performed a numerical simulation using a hydrostatic model to show the effect of terrain alone on airflow in the basin. A northwesterly wind of 4 m s^{-1} prescribed everywhere was employed upstream of the Coastal Range, and no surface radiative forcing was employed in their numerical simulation. A similar splitting of the gap jet was also predicted by their model. However, no well-organized vortices were predicted by their model either in the Sacramento Valley or in the San Joaquin Valley.

The lee vortex in the Sacramento Valley is associated with a positive potential temperature anomaly due to adiabatic warming of downward motion occuring over the northern Coastal Range (Fig. 2c). Because the flow is bounded and blocked by the northern boundary, only one strong vortex forms in the Sacramento Valley. In addition, the low pressure center is collocated with the Sacramento eddy, which is similar to the flow response accompanying the formation of the Taiwan mesoscyclone (Lin et al. 1992). When a hydrostatic, high–Froude number barotropic flow impinges on an isolated mesoscale topography, an upstream high and a leeside low will appear according to linear hydrostatic mountain wave theory (e.g., Smith 1979). Because of

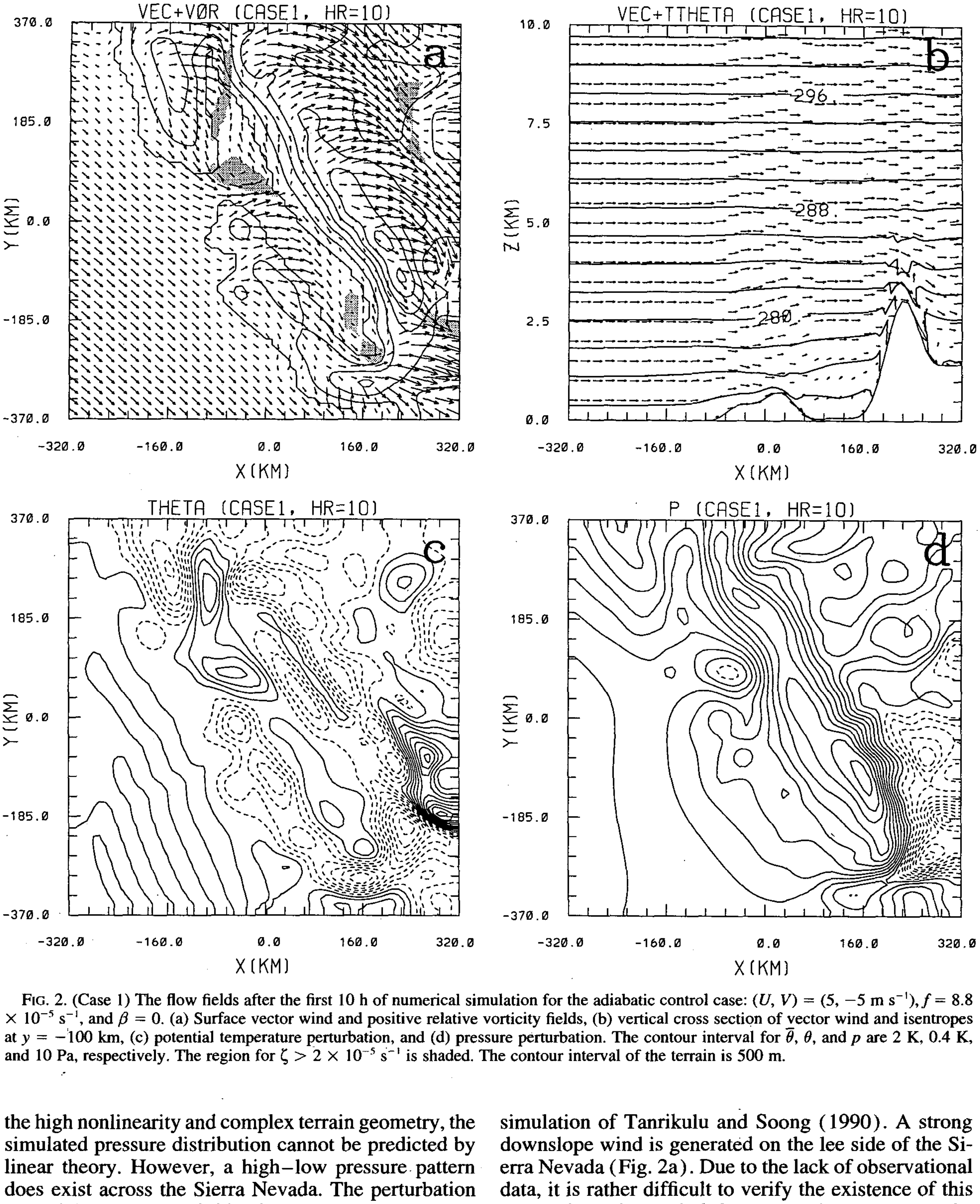

FIG. 2. (Case 1) The flow fields after the first 10 h of numerical simulation for the adiabatic control case: $(U, V) = (5, -5 \text{ m s}^{-1})$, $f = 8.8 \times 10^{-5} \text{ s}^{-1}$, and $\beta = 0$. (a) Surface vector wind and positive relative vorticity fields, (b) vertical cross section of vector wind and isentropes at $y = -100$ km, (c) potential temperature perturbation, and (d) pressure perturbation. The contour interval for $\bar{\theta}$, θ, and p are 2 K, 0.4 K, and 10 Pa, respectively. The region for $\zeta > 2 \times 10^{-5} \text{ s}^{-1}$ is shaded. The contour interval of the terrain is 500 m.

the high nonlinearity and complex terrain geometry, the simulated pressure distribution cannot be predicted by linear theory. However, a high–low pressure pattern does exist across the Sierra Nevada. The perturbation potential temperature field (Fig. 2c) also shows strong adiabatic cooling (warming) occurring on the upslope (downslope) side of the Coastal Range and Sierra Nevada due to adiabatic ascent (descent). The above results are also consistent with the adiabatic numerical simulation of Tanrikulu and Soong (1990). A strong downslope wind is generated on the lee side of the Sierra Nevada (Fig. 2a). Due to the lack of observational data, it is rather difficult to verify the existence of this strong downslope wind. However, the present results are consistent with the two-dimensional theories of severe downslope winds (e.g., Smith 1985; Durran 1986) and other numerical simulations (e.g., Tanrikulu and McNider 1992).

After the first 10 h during which time the simulation is adiabatic, a nocturnal radiative cooling is prescribed over the entire mountain area for the last 12 h of the simulations. Figure 3 shows the flow features at t = 16 h, 6 h after the cooling is turned on. With the addition of prescribed cooling, the air above the mountains becomes denser than its immediate environment. The resulting downslope drainage flow is evident over the northern Coastal Range and eastern slopes of the southern Coastal Range and Sierra Nevada. However, no strong draingage flow is simulated over the western slope of the Sierra Nevada near the valley center (Figs. 3a,b). The drainage flow may be weakened by the stronger southerly return flow from the Tehachapi Mountains, as evidenced by the sensitivity experiment of reducing the height of these mountains (Fig. 6). The splitting of the northwesterly jet in the central basin still occurs. The perturbation pressure associated with the jet is weaker (not shown) since the perturbation wind speed decreases. That is, when prescribed cooling is included, more of the drainage wind from the Coastal Range flows into the break. The cold air will increase the pressure and weaken the northwesterly jet. The mesoscale vortex in the Sacramento Valley moves farther to the east. In addition, the cyclonic circulation in the San Joaquin Valley strengthens when the southeasterly wind blowing from the foothills of the Sierra Nevada converges with the northwesterly wind from the central basin.

After cooling for 12 h (i.e., at the end of the 22-h control simulation), the katabatic wind is even stronger and is still confined within a thin layer above the surface over the northern and southern parts of the western slopes of the Sierra Nevada (Fig. 4a). The jet located at the gap of the Coastal Range at 10 h (Fig. 2a) and 16 h (Fig. 3a) is suppressed and replaced by a northerly downslope wind from the northern Coastal Range. The cyclonic vortex located in the southern end of the San Joaquin Valley at earlier times (Fig. 2a) strengthens and expands northward toward Fresno (Fig. 4a). This eddy is produced by the southeasterly wind along the foothills of the Sierra Nevada and the northwesterly wind from the Central Valley. Notice that the northward expansion of the Fresno eddy is partly due to the strong drainage flow occuring over the eastern slope of the southern Coastal Range and over the northern slope of the Tehachapi Mountains, while the positive vorticity maximum in the Sacramento Valley moves eastward to the foothills of the Sierra Nevada. The positive vorticity maximum in the San Joaquin Valley extends northward to encompass a larger elliptic-shaped area. The maximum vorticity associated with the Fresno eddy is 4.6×10^{-4} s^{-1}. There is a new region of positive vorticity located to the west of the northern Coastal Range, which is formed by the incoming northwesterly and the downslope drainage flow impinging on the western slope of the northern Coastal Range. The circulation associated with this new region of positive vorticity may extend vertically to a height of 500–1000 m (not shown). The Sacramento eddy moves farther northeastward to the foothills of the Sierra Nevada. High pressure covers most of the mountainous area due

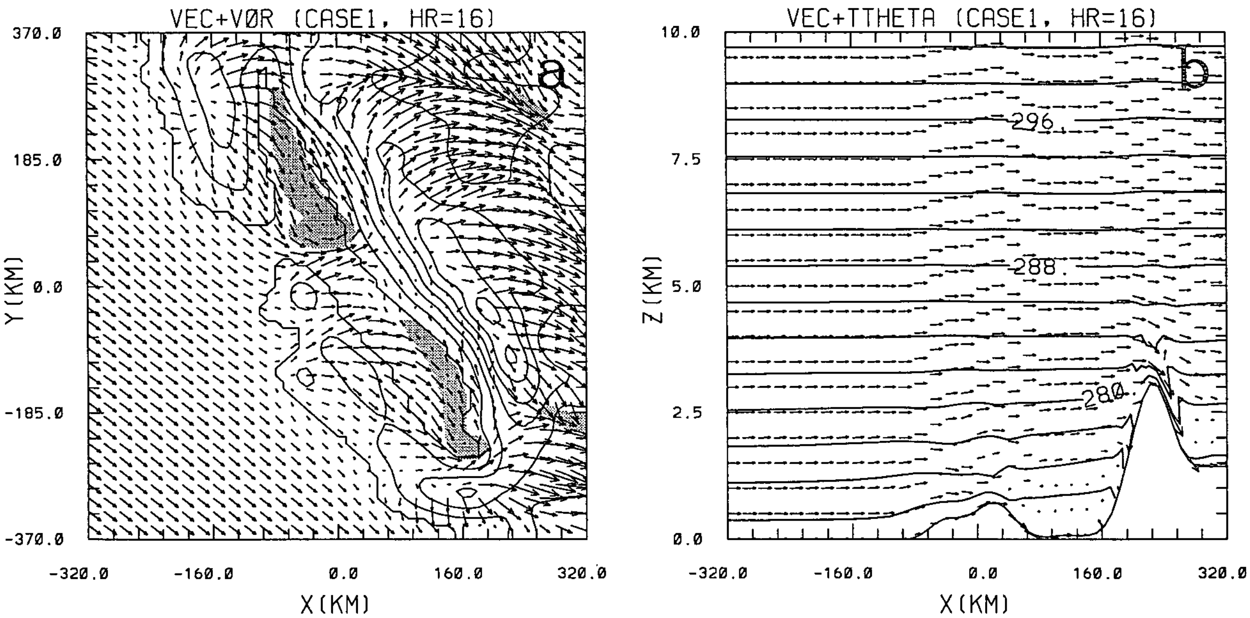

FIG. 3. Same as Fig. 2 except that prescribed cooling is activated for 6 h. The total simulation time is 16 h. (a) Surface vector wind and relative vorticity (shaded for $\zeta > 2 \times 10^{-5}$ s^{-1}) fields, and (b) vertical cross section of vector wind and isentropes at $y = -100$ km.

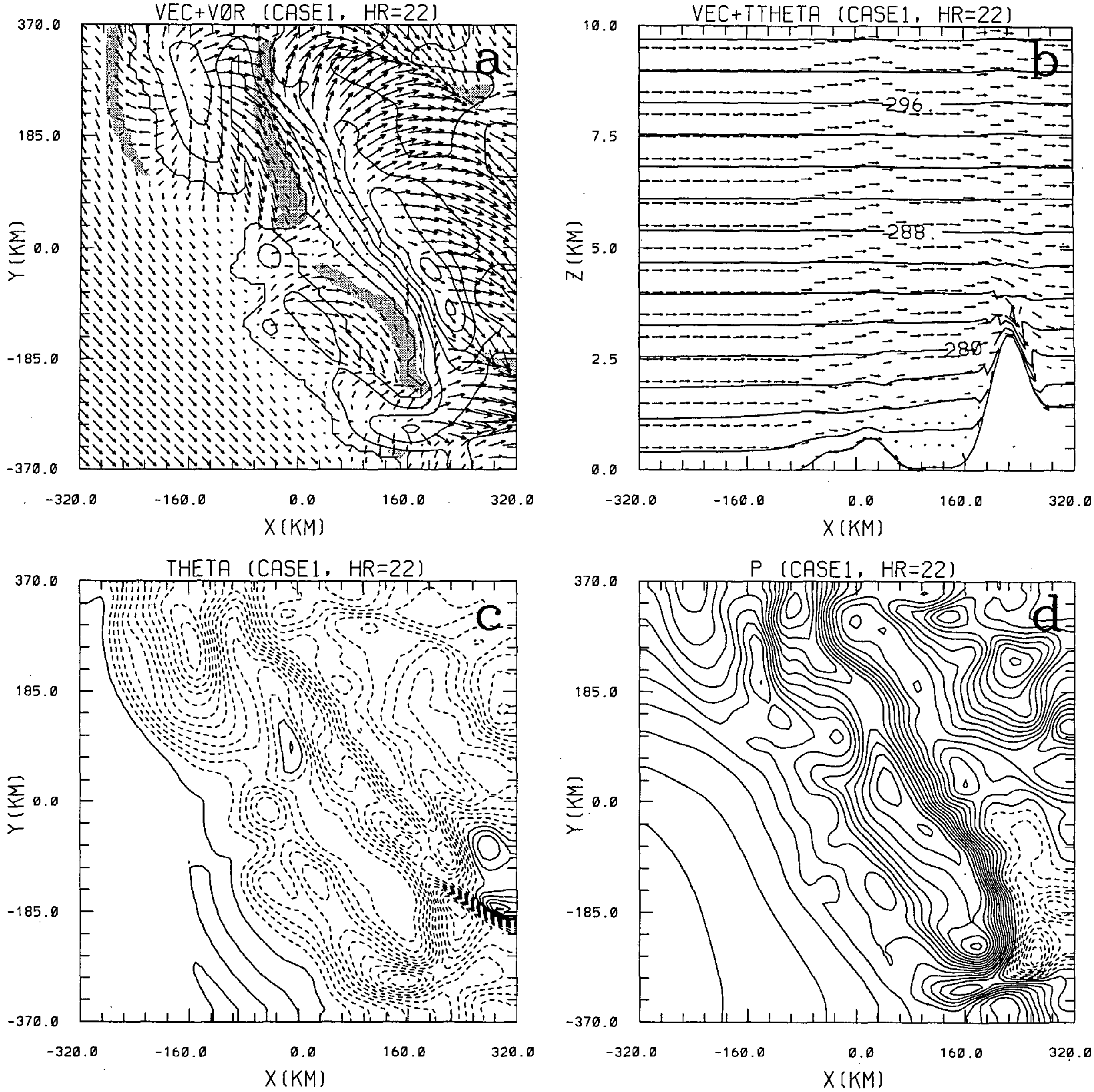

FIG. 4. Same as Fig. 2 except that the prescribed cooling is activated for 12 h. The total simulation time is 22 h. (a) Surface vector wind and relative vorticity (shaded for $\zeta > 2 \times 10^{-5}$ s^{-1}) fields, (b) vertical cross sections of vector wind and isentropes at $y = -100$ km, (c) potential temperature perturbation, and (d) pressure perturbation. The contour intervals for $\overline{\theta}$, θ, and p are 2 K, 0.4 K, and 10 Pa, respectively. The vorticity associated with the Fresno eddy in this case is 4.6×10^{-4} s^{-1}.

to the nocturnal cooling (Fig. 4c). Strong pressure and temperature gradients form across the relatively warm basin and the cold mountainous area (Fig. 4d). The primary effect of nocturnal radiative cooling contributing to the formation of the Fresno eddy is to strengthen and expand the cyclonic vortex farther to the north.

In summary, the simple numerical model adopted here is able to simulate the Sacramento eddy, the northwesterly jet at the gap of the Coastal Range, the Fresno eddy, and the associated drainage flow when prescribed cooling is applied. The formation of the Fresno eddy occurs when a low–Froude number northwesterly wind blows into the Central Valley and encounters the southerly return flow from the Tehachapi Mountains. The Fresno eddy strengthens and expands northward in the presence of nocturnal radiative cooling.

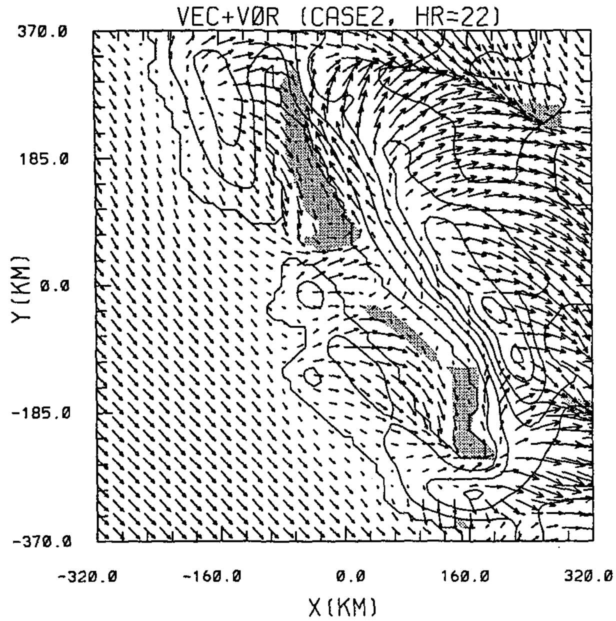

FIG. 5. (Case 2) The vector wind and relative vorticity (shaded for $\zeta > 2 \times 10^{-5}$ s^{-1}) fields at 22 h for the case without nocturnal radiative cooling. The vorticity associated with the Fresno eddy in this case is 4×10^{-4} s^{-1}.

4. Sensitivity experiments

Based on the above control experiment, we make a series of sensitivity experiments to help understand the formation dynamics of the Fresno eddy and the flow patterns in the Central Valley. The following parameters will be varied in this section in order to examine the individual dynamical processes associated with variations in (a) the diabatic forcing, (b) the height of the southern boundary (Tehachapi Mountains), (c) the Froude number, (d) the impinging angle of the basic flow, (e) the Coriolis parameter, and (f) the β effect.

a. Effect of diabatic cooling (case 2)

After a quasi-steady-state flow established during the first 10 h of simulation time, the flow is still kept adiabatic throughout the remaining 12 h in this experiment in order to determine the effect of nocturnal radiative cooling on the development of the Fresno eddy simulated during the control experiment. Figure 5 shows the flow fields at the end of this 22-h adiabatic simulation. In general, the overall flow pattern is similar to that of the control case. The pressure gradient between the San Joaquin Valley and the surrounding mountains is decreased from that simulated by the control case (not shown). The northwesterly jet in the central basin is similar to that in the control case at 10 h (compare with Fig. 2a), and only a weak southeasterly wind from the foothills of the Sierra Nevada blows into the basin. As a consequence, the circulation associated with the Fresno eddy is weaker than the control case at the same time (Fig. 4a). Comparing with the 16-h results (Fig. 3a), this indicates that nocturnal radiative cooling plays an important role in strengthening the temperature (pressure) contrast between the cold mountain and warm basin air and, therefore, causes a stronger southeasterly wind to blow into the San Joaquin Valley. Therefore, we may conclude that *nocturnal radiative cooling strengthens the mesoscale circulation associated with the Fresno eddy.*

b. Effects of the Tehachapi Mountains (case 3)

In this experiment, all prescribed model parameters are the same as those in the control case except that the southern boundary (Tehachapi Mountains) of the San Joaquin Valley is lowered to a constant height of 500 m. Figure 6 shows the surface vector wind and vorticity fields at $t = 22$ h for this simulation. The flow pattern in the Sacramento Valley is very similar to that in the control case. However, due to a weaker blocking effect by the lower mountains at the southern end of the valley, the wind can easily pass through the San Joaquin Valley. Since the return flow from the Tehachapi Mountains has been eliminated, no Fresno eddy is able to form in this case. The positive relative vorticity field is much weaker, since most of the air parcels flow out of the San Joaquin Valley over the lowered Tehachapi Mountains, which therefore reduces the southerly return flow along the western slope of the Sierra Nevada. Notice that the downslope drainage flow is very strong over the western slope of the Sierra Nevada. Compared

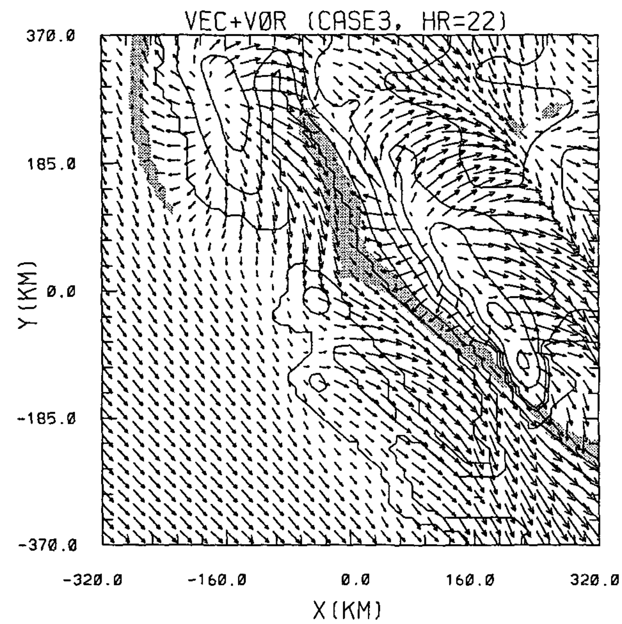

FIG. 6. (Case 3) Same as Fig. 4 except for the case where the height of the Tehachapi Mountains at the southern end of the San Joaquin Valley has been reduced to a uniform value of 500 m.

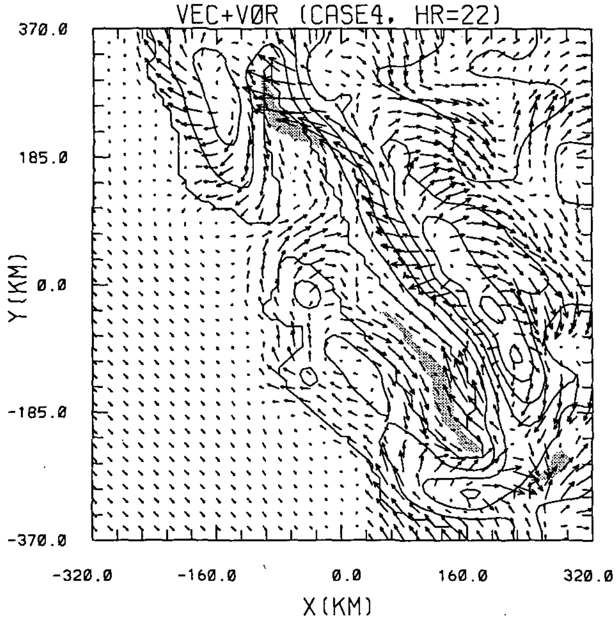

FIG. 7. (Case 4) Same as Fig. 4 except for a case with a weaker basic wind $(U, V) = (1, -1 \text{ m s}^{-1})$. The vorticity associated with the Fresno eddy in this case is $3.1 \times 10^{-4} \text{ s}^{-1}$.

with the control case (Fig. 4a), the southerly return flow from the Tehachapi Mountains tends to weaken the drainage flow. *These results indicate that the return flow from the southern boundary of the San Joaquin Valley plays an essential role and is therefore a primary formation mechanism for the Fresno eddy.*

c. Effects of ambient wind speed (case 4)

To examine the sensitivity of the flow response to ambient wind speed, a case with weaker northwesterly basic wind $(U, V) = (1, -1 \text{ m s}^{-1})$ was performed. The Froude number (U/Nh) associated with this basic flow is in the range of 0.05–0.14, which is much smaller than the control case. Because of the small Froude number, it is difficult for the wind to pass directly over the mountains since the air parcels do not possess enough kinetic energy to do so. The incoming wind almost flows completely around the Coastal Range, the recirculated flow along northern coastal range is decreased, and the downslope flow over the western slope of the Sierra Nevada increases during the first 10 h of simulation (not shown). Figure 7 shows the flow fields at 22 h, that is, 12 h after the prescribed cooling is activated. The Sacramento eddy remains on the lee side of the northern Coastal Range but moves farther east in the control case (Fig. 4a). Similar to the control case, a reversed flow and stagnation points form upstream of the Coastal Range. This results in an elongated, elliptically shaped cyclonic vortex north of the San Francisco Bay area. The vorticity maximum in the Sacramento Valley is located farther to the north, compared with the control case, while the vorticity maximum in the San Joaquin Valley expands to the north, similar to the control case, but is located in the central portion of the valley due to the relatively stronger downslope wind present over the western slope of the Sierra Nevada. The vorticity is weaker than that of the control case since the incoming basic wind is much weaker. The northwesterly jet at the central basin in the control case becomes a westerly jet in this case. The Fresno eddy is shifted slightly westward from that in the control case by the stronger downslope wind and southerly return flow from the Tehachapi Mountains at the southern boundary. The circulation associated with the Fresno eddy is weaker (maximum vorticity of $4 \times 10^{-4} \text{ s}^{-1}$, compared to $4.6 \times 10^{-4} \text{ s}^{-1}$ of the control case) and the circulation is still confined to a shallow layer. An experiment with a larger wind speed (Froude number) is also conducted. The results also show in this case that a weaker Fresno eddy forms in the San Joaquin Valley. *Therefore, we may conclude that the upstream ambient wind speed may affect the circulation strength of the Fresno eddy.*

d. Effects of wind direction (case 5)

To test the sensitivity of the flow response to the basic wind direction, we change the flow direction from northwesterly to westerly, while maintaining the same wind speed (7 m s^{-1}) and Froude number used in the control run (case 1). Other model parameters are kept the same. Figure 8 shows the flow fields at 22 h for this case. The upstream westerly flow becomes southwest-

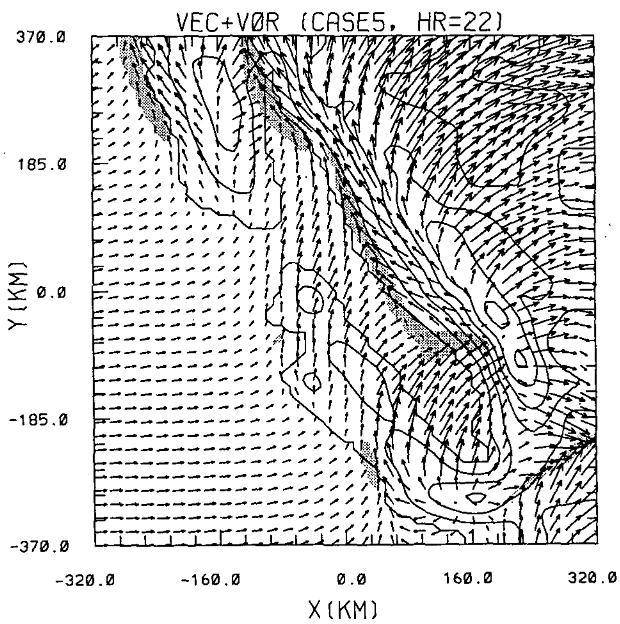

FIG. 8. (Case 5) Same as Fig. 4 except for a westerly wind case with $(U, V) = (7, 0 \text{ m s}^{-1})$.

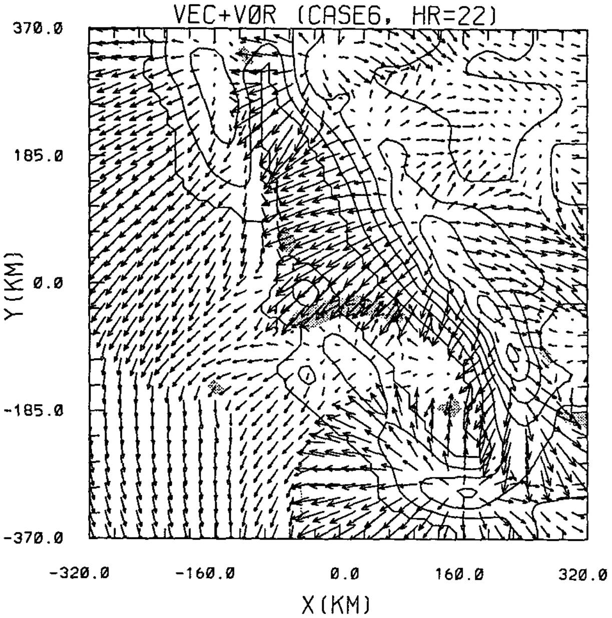

FIG. 9. (Case 6) Same as Fig. 4 except for a case with no planetary rotation ($f = 0$).

erly as it reaches the Coastal Range (Fig. 8). This deflection is due to the orographically induced high pressure over the upslope side of the Coastal Range (e.g., see Smith 1979). More flow is able to pass over the mountains, and stronger adiabatic cooling (warming) on the upwind (downwind) side of the mountains occurs due to the larger impinging angle between the basic wind and the Coastal Range. The Sacramento eddy is not able to form in this particular case. The northwesterly jet in the central basin simulated by the control case is now totally absent. The drainage flow over the western slope of the Sierra Nevada cannot blow into the San Joaquin Valley since it is strongly blocked, and no southeasterly wind occurs. A relatively strong southwesterly wind prevails throughout the entire basin area, and the Fresno eddy is not simulated.

We have also conducted a case with a west-northwesterly incoming wind with the same basic wind speed as the control case, and the simulated flow field (not shown) appears to be an average between the westerly and northwesterly wind cases. That is, the Fresno eddy is stronger than that in the case with westerly wind but weaker than the control case. *Therefore, we may conclude that the wind direction plays an important role in forming the Fresno eddy. A northwesterly wind flow appears to be more favorable for the formation of the mesoscale circulation.*

e. *Effect of planetary rotation (case 6)*

In this experiment, the Coriolis parameter f is set to 0. Other flow parameters are kept the same as those in the control case. Notice that the Rossby number (U/fL) associated with the flow in the control case falls into the range of 0.78–0.9, where L is taken to be the horizontal scale of the Sierra Nevada and the Coastal Ranges (i.e., 100 and 80 km, respectively).

Figure 9 shows the flow fields at 22 h for this case. The stagnation point upstream of the northern Coastal Range, the Sacramento eddy, and the northwesterly jet in the central basin are absent. The flow field is totally dominated by the drainage flow that flows down from the mountain peaks. A region of divergence occurs in the San Joaquin Valley. Neither the Sacramento eddy nor the Fresno eddy is able to form in this particular case.

Because the Rossby number is of $O(1)$, the circulation system in the Central Valley falls into the flow regime in which the Coriolis effect *cannot* be neglected. *In the absence of planetary rotation, the Fresno eddy is not simulated, and the flow structures in the valley are dominated by the drainage flow induced by the prescribed cooling, which flows down from the mountain peaks.*

f. *β effect (case 7)*

We activate the β terms in the governing equations in this particular experiment. The value of β is taken to be 1.8×10^{-11} m s^{-1}. Figure 10 shows the surface vector wind at 22 h for this case. The circulation associated with the Fresno eddy is slightly stronger than that produced by the f-plane control case (Fig. 4a). The

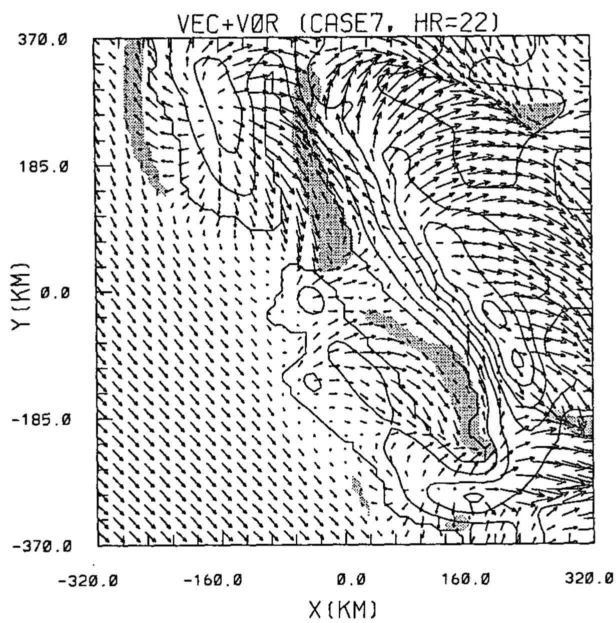

FIG. 10. (Case 7) Same as Fig. 4 except for a case with the β effect included. The value of β is taken to be 1.8×10^{-11} m^{-1} s^{-1}. The vorticity associated with the Fresno eddy in this case is 5.2×10^{-4} s^{-1}.

overall flow pattern in the basin shows no significant differences from the control case (Fig. 4a), which is performed on an f plane. Therefore, the horizontal scale of the simulated mesoscale circulations is large enough to have a pronounced rotational effect but not large enough to have a pronounced β effect. *From this experiment, we may conclude that the β effect plays a negligible role in the formation and intensification of the Fresno eddy.*

5. Conclusions

In this study, we have conducted a series of numerical experiments to investigate the flow circulations in the Central Valley and the formation mechanisms of the Fresno eddy. A smoothed topography has been used in a simple three-dimensional, terrain-following, hydrostatic model. We have found the following.

- Under an adiabatic northwesterly, low–Froude number flow over the Central Valley, two cyclonic mesoscale vortices form in the basin. One is located on the lee side of the northern Coastal Range, while the other is located in the southern end of the San Joaquin Valley. The first may be identified as the Sacramento eddy, while the second may be identified as the Fresno eddy, even though the Fresno eddy is located slightly to the south of Fresno, California. The formation of the Sacramento eddy may be explained by either the generation of potential vorticity (Smith 1989) or baroclinically generated vorticity (Smolarkiewicz and Rotunno 1989) along the lee slope in a low–Froude number flow. The Sacramento eddy may also be classified as a lee mesocyclone since it is collocated with a lee mesolow (Lin et al. 1992). In addition, a northwesterly jet forms at the gap of the Coastal Range due to the channeling effect.
- The Fresno eddy forms when the low–Froude number northwesterly flow meets the return flow from the Tehachapi Mountains in a rotating fluid system. This mesoscale eddy is strengthened and expands farther to the north by the influence of nocturnal radiative cooling. The northwesterly jet at the valley center, the southeasterly wind from the foothills of the Sierra Nevada, and the blocking effect due to the Tehachapi Mountains all play important roles in the formation of the Fresno eddy. The Sacramento eddy moves eastward to the foothills of the Sierra Nevada, and the jet at the gap of the Coastal Range is suppressed when the effects of nocturnal radiative cooling are present in the numerical model.
- The nocturnal drainage flow over the western slope of the Sierra Nevada is weakened by the southerly return flow from the Tehachapi Mountains. Our numerical simulations indicate that in the absence of nocturnal diabatic cooling the Fresno eddy still forms but is weaker and is located near the southern end of the San Joaquin Valley.
- The upstream Froude number (U/Nh) and flow direction have been varied according to the available observational data. The Fresno eddy will form under a northwesterly flow characterized by a small Froude number. Suitable incoming flow speeds and directions are among the major factors in determining the formation and circulation strength of the Fresno eddy.
- The return flow from the southern end (the Tehachapi Mountains) of the San Joaquin Valley plays an essential role in the formation of the Fresno eddy.
- The Fresno eddy does not form in the absence of the planetary rotation.
- The β effect plays a negligible role in the formation of the Fresno eddy.

The mesoscale flow circulation in the Central Valley is extremely complicated due to the combined effects of complex orography and nocturnal radiative cooling. Our results provide insight into the basic flow dynamics in the basin and important factors contributing to the formation of both the Fresno and Sacramento eddies. To investigate specific, unresolved details about the mesoscale flow patterns, more realistic boundary layer processes and a nonuniform vertical profile of the Brunt–Väisälä frequency that characterizes the elevated marine inversion should be considered in future studies.

Acknowledgments. Discussions with Drs. S. Tanrikulu and R. P. Weglarz are highly appreciated. The authors also want to thank H. Bowden for help plotting Fig. 1a. This work is partially supported by the NASA Grant NAG 5-1790 and NSF Grant ATM-9224595. Portions of the numerical computations were performed on the CRAY Y-MP supercomputer located at the North Carolina Supercomputer Center and the NCSU FOAM RISC workstations, which are sponsored by an IBM equipment grant.

REFERENCES

Asselin, R. A.,1972: Frequency filter for time integration. *Mon. Wea. Rev.*, **100**, 487–490.

Barr, S., and M. Orgill, 1989: Influence of external meteorology on nocturnal valley drainage winds. *J. Appl. Meteor.*, **28**, 497–517.

Blumenthal, D. L., T. B. Smith, D. E. Lehrman, R. A. Rasmusen, G. Z. Whitten, and R. A. Baxter, 1985: Southern San Joaquin Valley Ozone Study. Final Rep. ST199092-981-D, California Air Resources Board, Sacramento, CA.

Crook, N. A., T. L. Clark, and M. W. Moncrieff, 1990: The Denver cyclone. Part I: Generation in low Froude number flow. *J. Atmos. Sci.*, **47**, 2725–2742.

Doran, J. C., 1990: The effect of ambient winds on valley drainage winds. *Fifth Conf. on Mountain Meteorology*, Boulder, CO, Amer. Meteor. Soc., 283–288.

Durran, D. R., 1986: Another look at downslope windstorms. Part I: On the development of analogs to supercritical flow in an infinitely deep, continuously stratified fluid. *J. Atmos. Sci.*, **43**, 2527–2543.

Horst, T. W., and J. C. Doran, 1986: Nocturnal drainage flow on simple slopes. *Bound.-Layer Meteor.*, **34**, 263–286.

——, and ——, 1988: The turbulence structure of nocturnal slope flow. *J. Atmos. Sci.*, **45**, 605–616.

Kessler, R. C., and S. G. Douglas, 1991: A numerical study of mesoscale eddy development over the Santo Barbara channel. *J. Appl. Meteor.,* **30,** 633–651.

King, C. W., P. H. Gudiksen, and C. A. Russell, 1990: Sodar-derived nocturnal drainage flow classifications. Preprints, *Fifth Conf. on Mountain Meteorology,* Boulder, CO, Amer. Meteor. Soc., 244–249.

Klemp, J. B., and D. K. Lilly, 1978: Numerical simulation of hydrostatic mountain waves. *J. Atmos. Sci.,* **35,** 78–107.

Lin, Y.-L., N.-H. Lin, and R. P. Weglarz, 1992: Numerical modeling studies of lee mesolows, mesovortices, and mesocyclones with application to the formation of Taiwan mesolows. *Meteor. Atmos. Phys.,* **49,** 43–67.

Neff, W. D., J. M. Wilczak, and C. W. King, 1992: Development and evolution of the Fresno eddy as observed with a boundary layer profiler. Preprints, *Sixth Conf. on Mountain Meteorology,* Portland, OR, Amer. Meteor. Soc., 233–235.

Orgill, M., J. D. Kincheloe, and R. A. Sutherland, 1990: Mesoscale influences on nocturnal valley drainage winds in western Colorado valleys. Preprints, *Fifth Conf. on Mountain Meteorology,* Boulder, CO, Amer. Meteor. Soc., 239–243.

Ruffner, J. A., and F. E. Bair, 1985: *Weather of U.S. Cities.* Vol. 1. Gale Research, 609 pp.

Seaman, N. L., and David R. Stauffer, 1994: The Fresno eddy: Numerical investigation of a mesoscale wind feature of the San Joaquin valley using the Penn State/NCAR MM5. Preprints, *Sixth Conf. on Mesoscale Processes,* Portland, OR, Amer. Meteor. Soc., 572–575.

Shapiro, R., 1970: Smoothing, filtering, and boundary effects. *Rev. Geophys. Space Phys.,* **8,** 359–387.

Smith, R. B., 1979: The influence of mountains on the atmosphere. *Advances in Geophysics,* Vol. 21, Academic Press, 87–230.

——, 1985: On severe downslope winds. *J. Atmos. Sci.,* **42,** 2597–2603.

——, 1989: Comments on "Low Froude number flow past three-dimensional obstacles. Part I: Baroclinically generated lee vortices". *J. Atmos. Sci.,* **46,** 3611–3613.

Smolarkiewicz, P. K., and R. Rotunno, 1989: Low Froude number flow past three-dimensional obstacles. Part I: Baroclinically generated lee vortices. *J. Atmos. Sci.,* **46,** 1154–1164.

——, R. Rasmussen, and T. L. Clark, 1988: On the dynamics of Hawaiian cloud bands: Island forcing. *J. Atmos. Sci.,* **45,** 1872–1905.

Sun, W.-Y., J.-D. Chern, C.-C. Wu, and W.-R. Hsu, 1991: Numerical simulation of mesoscale circulation in Taiwan and surrounding area. *Mon. Wea. Rev.,* **119,** 2558–2573.

Tanrikulu, S., and S.-T. Soong, 1990: A numerical simulation of the summer wind flow pattern in the central valley of California. Preprints, *Fifth Conf. on Mountain Meteorology,* Boulder, CO, Amer. Meteor. Soc., 92–97.

——, and R. T. McNider, 1992: Analysis of mesoscale wind patterns in the San Joaquin Valley of California during a SJVAQS/AUSPEX 1990 intensive measurement period. Preprints, *Sixth Conf. on Mountain Meteorology,* Portland, OR, Amer. Meteor. Soc., 228–232.

Weglarz, R. P., 1994: Three-dimensional geostrophic adjustment of homogeneous and continuously stratified atmospheres with application to the dynamics of midlatitude jet streaks. Ph.D. thesis, North Carolina State University, 414 pp.

Whiteman, C. D., 1990: Observations of thermally developed wind systems in mountainous terrain. *Atmospheric Processes over Complex Terrain,* W. Blumen, Ed., Amer. Meteor. Soc., 323 pp.

Wilczak, J. M., M. L. Cancillo, and C. W. King, 1992: Observations of mesoscale flows in northern California using an array of wind profilers. Preprints, *Sixth Conf. on Mountain Meteorology,* Portland, OR, Amer. Meteor. Soc., 222–227.